The Effects of Fluctuating Operation on Reverse Osmosis Membranes

University of South Australia

Technische Universiteit Delft

International Centre of Excellence in Water Resources Management

The Effects of Fluctuating Operation on Reverse Osmosis Membranes

Brett Ibbotson

For the degree of

Master Water Resource Management

Date of submission: 12th February 2010

University of South Australia
Delft University of Technology

Abstract

Directly coupling renewable energy to reverse osmosis may be the most cost effective solution to supply potable water to remote and isolated areas that lack infrastructure and safe drinking water. These systems do not use batteries but rather operate only when sufficient energy is available and store any excess energy as water. Since reverse osmosis membranes are designed to be operated for continuous periods under constant power, it has been unclear how the fluctuating operation will affect the performance of the membranes.

In these experiments, a small-scale reverse osmosis unit (maximum production 8 m^3/day) was set up in the laboratory to continually recycle and treat a reservoir of artificial seawater (32 800 mg/L NaCl). The power of the high pressure pump feeding the reverse osmosis membranes is fluctuated corresponding to inputs of real wind data entered through an automated computer system. Measurements of pressure, permeate production and conductivity were continually recorded and used to determine if there were changes in the membrane permeability coefficient and salt rejection of the membrane resulting from fluctuating operation.

After more than 650 hours of fluctuating operation, no deterioration of reverse osmosis membrane performance was observed.

Preface

This research was conducted as part of the *Drinking with the Wind* project of TU Delft which has now led into the *Drinking with the Sun* project. Both these projects aim to couple renewable energy to reverse osmosis using the most efficient and cost effective methods possible. All work presented in this report is the authors own work except where due acknowledgement is given.

The author conducted the research whilst on exchange from the University of South Australia, participating in the International Centre of Excellency in Water Resource Management (ICEWaRM) European Union/Australian exchange program. Both organizations provided much appreciated funds to facilitate the exchange.

The author also wishes to thank TU Delft for hosting him on the exchange and for funding the research, and those who helped design and construct the experimental set-up.

CONTENTS

List of Illustrations

List of Tables

List of Abbreviations

RO	reverse osmosis
RES	renewable energy source
FW	fresh water
BW	brackish water
SW	sea water
HPP	high pressure pump
WECS	wind energy converter system
TDS	total dissolved solids
PV	photo voltaic
DW	demineralized water
SDM	solution diffusion model
WHO	world health organization

List of Symbols

Qs = salt flux (g/s)

K_2 = membrane salt permeability (m/s)

A = area membrane (m^2)

C_f = concentration in feed (g/m^3)

γ = recovery

F = flush ratio

V_f = volume used for flush (L)

V_c = volume of water retained in the Spectra LB 1800 when it is dormant (L)

V_m = volume of water in membranes (L)

R = rejection

c_p = concentration in permeate (g/m^3)

Q = permeate flow (m^3/s)

K = membrane permeability coefficient (m)

μ = viscosity of water (Pa/m^2)

ΔP = membrane pressure inlet – membrane pressure outlet (Pa)

$\Delta \pi$ = osmotic pressure in membrane (Pa)

$Q_{av.\ prod}$ = average permeate flow from all production tests (m^3/s)

$K_{av.\ DW}$ = average membrane permeability coefficient from all demineralized water tests (m)

$\Delta P_{av.prod}$ = average pressure for all production tests (Pa)

π_m = osmotic pressure at membrane surface (Pa)

π_f = osmotic pressure of feed water (artificial seawater) (Pa)

β = concentration polarization

1. INTRODUCTION

1.1 Background

The growing demand for potable water, along with the increased awareness of carbon emissions from the burning of fossil fuel's has led to interest in the combination of desalination with renewable energy. It has long been suggested that small-scale renewable energy powered desalination systems may be the most cost effective solution for providing potable water to remote and isolated communities where access to an electricity grid and proper infrastructure are lacking (Houcine et al., 1999).

The most power-efficient method of desalination is reverse osmosis (Kalogirou, 2005) which also has the advantages of being modular in nature and compact in size. The coupling of reverse osmosis (RO) to a renewable energy source (RES) has been examined in a number of papers from as far back as 1979 (Petersen et al., 1979). For a recent and comprehensive overview of the 'state-of-the-art' in membrane processes for desalination using renewable energy, see Charcosset (2009) and for a recent review of all desalination processes using RES see Eltawil et al. (2009).

The nature of renewable energies means that generally they fluctuate over time while traditionally RO plants have been designed to operate under constant and continued conditions. This creates two options for the design of a plant combining RO with a RES; either store and regulate the power supplied to the RO unit (most commonly with the use of batteries), or operate the RO under fluctuating conditions. The former approach has been presented by numerous authors; Alawaji et al. (1995) described a prototype of an autonomous system built in Saudi Arabia that included Photovoltaic(PV)-powered water pumping as well as RO; Infield (1997) developed models to optimize battery storage capacities and reverse osmosis operating pressures; Herold et al. (1998) evaluated an RO/PV system with batteries but reports production costs of $\$16/m^3$; Ahmad and Schmid (2002) examined the suitability of sites in Egypt for the coupling of RO and PV for brackish water desalination; Tzen et al. (1998) presented a case study for a small Moroccan fishing village with an economic evaluation of PV powered RO; Weiner et al. (2001) used wind and solar power to charge a battery bank for RO; Al Suileimani and Nair (2000) present a dual module PV/RO system operating for 3 years in Oman and calculated it to be more cost effective than a diesel-run system if considered over a 20 year plant life.

Perhaps a better approach is to operate the plant when energy is available. In such systems, excess energy can be stored as produced permeate in a tank, rather than storing energy in batteries. The advantages of this are:

1. Reduced capital and maintenance costs associated with batteries (Park et al., 2009).
2. Reduction of the environmental impact and disposal problems associated with batteries.
3. An increase in the efficiency of the desalination system; charge in/charge out of a typical lead deep cycle battery is 75-80% (Richards et al., 2008). Overall system losses are even greater if considering a wind powered system that needs to convert kinetic energy to electrical energy for battery storage, then back to kinetic energy for reverse osmosis.
4. A more simplified system that affords less maintenance and greater reliability in remote areas.

This report looks with more detail into the operation of directly coupled RO/RES desalination systems.

1.2 Wind Energy

Wind energy is an obvious renewable energy source for sea water (SW) desalination since consistent high wind speeds are often associated with coastal locations. Locations such as those along the Red Sea and Mediterranean are ideal candidates for this technology, with their combination of arid on-land conditions and high year-round wind speeds (Ahmed Shata and Hanitsch, 2008) making this perhaps the most cost effective of the renewable energy sources (Gilau and Small, 2008).

Kiranoudis et al. (1997) presented a mathematical-based report on the exploitation of wind energy for RO with regards to plant design. The conclusion was that autonomous operation was possible, but required over sizing of equipment when compared to a conventionally powered system of a given production to compensate for the fluctuating operation. Lui et al. (2002) used a directly coupled RO/wind energy system for the treatment of brackish water (BW) that included a pressure stabilizer and feedback control. Results were reported for only two separate days of trial, one on a day of relatively high constant wind speeds, the other with slightly lower and more fluctuating wind speeds. Interestingly, the reported rate of salt rejection and permeate recovery were better for the day with greater fluctuation in wind speeds, although this was most likely due to the lower TDS in the feed water for this trial. Maintaining the same feed water quality for both trials would have made for a more useful comparison. This same system was later used for the treatment and nutrient recovery of aquaculture waste water (Lui et al., 2007).

Heijman et al. (2009) described an entirely mechanical system using a multivaned windmill mechanically coupled to a high pressure pump (HPP) and energy recovery device for RO. Miranda and Infield (2002) presented modeling for a directly coupled system powered by a 2.2 kW wind turbine. The model suggests good energy efficiency of 3.5 kWh/m^3 however the statement is made that very little is known about the consequences of variable operation on membrane performance. It is suggested that mechanical fatigue of components can occur and that the lifetime of the RO elements may be shortened and performance impaired.

Another option for operation without batteries exploits the modular nature of RO such that a number of RO units can be used for a given renewable energy source and brought into production as more energy becomes available. A prototype of such a system is described by Carta et al. (2003); this system is quite elaborate in design and requires a high level of computer programming and control. It is one of the largest directly coupled RO/RES prototypes cited in the literature at a potential of 200 m^3/day. The WindDeSalter® technology is also an interesting application of directly coupled RO with wind energy. This system utilizes offshore WECS (wind energy converter systems) and proposes containing the RO module, as well as all supplementary water treatment and storage components within these large ocean-built WECS towers (Witte et al., 2003).

1.3 Photovoltaic

There have been several studies looking at coupling photovoltaic power to desalination; direct coupling was trialed in the early 1980's (Keefer et al., 1985). Thomson and Infield (2002) presented a model for a seawater PV/RO system, based on readily available components, that calculated the production cost of potable water to be £2/m^3. Interestingly they included in their calculations the replacement of membranes every 12 months, which would generally be considered quite a short life-span for a RO membrane. A second paper from these authors, published around the same time, gives further details of the system's components and cites a specific energy consumption of 3.5 kWh/m^3 (Thomson et al., 2002). A prototype of this directly coupled PV/RO seawater desalination unit was built and tested in the UK. Results were inconclusive since the permeate produced was over the guideline value of 500 mg/L TDS.

However, the authors make reference to the fact that the prototype was constructed with components that were not optimal as proposed in the model. Additionally the regular cloud cover present at the testing site in the UK was not ideal. Performance could have been increased in a more suitable location closer to the equator and with the more optimal components (Thomson and Infield, 2005). Another study compared a small-scale PV/RO system run with battery storage to a directly coupled system. It was found that the battery-based system performed better with regards to permeate production and quality, however the water production costs were 8 Euro/m^3 compared to 7.8 Euro/m^3 in favour of the directly coupled system (Mohamed et al., 2008).

1.4 Other RES/RO

Other interesting studies regarding autonomous RO desalination with RES include the use of a low temperature solar Rankine cycle system (Manolakos et al., 2005) and the use of wave energy and a hydraulic accumulator (Folley et al., 2008). The later model proposed exceptionally good efficiency of 1.85 kWh/m^3 however it raised the question of the effect on membrane life during fluctuating operation and subsequent economic considerations.

1.5 Membrane Performance

While other studies have looked at the performance of thin film composite reverse osmosis membranes under fluctuating temperature (Abdel-Jawad et al., 2001) and feed water quality (Lee et al., 2003), this study will focus on the effects of fluctuating operation. While it has been assumed by some authors that fluctuating operating conditions will decrease the life of RO membranes, there is little data to date that confirms this assumption. Herold and Neskakis (2001) state in their paper discussing the optimal battery operation cycle for RO coupled to PV, that reducing the plant start-up events per day "is an important factor for the lifetime expectancy of the membranes of the RO plant, which are best operated continuously at a constant feed pressure to avoid structural membrane damage"; however, they provide no evidence to support this statement.

Mohamed et al. (2006) described a small-scale laboratory experiment where a single membrane module with capacity of 1.7m^3/day was run for 80 hours with 2 idle periods. Graphs were presented comparing permeate conductivity and membrane inlet pressure over time which demonstrated that a slight reduction in feed pressure led to a high increase in the permeate conductivity, with a greater increase during the idle periods. The objective of that paper was focused more on the performance of a hydraulic energy recovery unit with little detail being provided on the membrane performance. A performance loss of 7% per annum was reported by Harrison (1996) for a brackish water (BW) RO system coupled to a RES. However no further explanation was given.

De Munari et al. (2009) conducted field trials in Coober Pedy, South Australia on three separate days with a small-scale BW RO system directly coupled to solar-tracking PV RES. Three separate tests were conducted using two different sources of saline groundwater; the first in batch production with low salinity water (EC 7.4 mS.cm^{-1}), the second in continuous production with low salinity water and the third in batch production with high salinity water (EC 25.6 mS.cm^{-1}). Unfortunately the capacity of the system was unable to provide the pressures and flow necessary to satisfactorily treat the high salinity water, with the permeate exceeding quality targets. Both tests using low salinity water produced permeate with TDS below the target of 500 mg/L and an economic assessment suggested that the diesel-powered RO plant currently supplying potable water to Coober Pedy, would save up to AU$2.4 million over 20 years if run directly by PV (De Munari, et al., 2009).

Similarly Richards and co-authors (2008) present data from field trials conducted in Central Australia using the same system as De Munari to treat BW, however the trials used different types of membrane. Performance was satisfactory for all but one of the membranes tested and it was reported that PV power fluctuations of up to 50% during the day do not compromise the ability of the system to produce permeate below the guideline value of 500 mg/L TDS (Richards et al., 2008). It is interesting to note that the guideline value of 500 mg/L TDS is based more on aesthetic properties rather than health considerations; in some areas such as central Australia, the population prefers the taste of water with greater than 500 mg/L TDS (Schafer et al., 2007). This could potentially allow for a greater operational range of a desalination system (Werner and Schafer, 2007).

Two studies by Al.-Bastaki and Abbas (1998 and 1999) looked at cyclic operation of RO desalination using spiral wound membranes and artificial brackish water (10 000 ppm NaCl). They ran asymmetrical and symmetrical pressure waves with fluctuations of between 5 and 10 bar and time periods of between 5 and 15 minutes for an experimental duration of 30 minutes. Both studies observed an increase in permeate production as a result of the cyclic operation with increases of 13% for symmetrical pressure waves and 6.5% for asymmetrical pressure waves when compared to steady-state production. This increase was attributed to the disturbance of fouling and the concentration polarization layer on the membrane surface as a result of the cyclic operation. These tests were only conducted for short periods so provide no information on potential long term effects of the pressure fluctuations. Subiela et al. (2009) comments in a review of a number of battery-based RO/RES desalination systems used in projects undertaken by the Canary Islands Institute of Technology, that flow fluctuations created by a variable power supply could be favourable in terms of reducing the concentration polarization in RO, depending on the frequency and amplitude of the fluctuations.

One of the few studies that was found relating to this current research using high salinity feed water, was that conducted by Abufayed (2003) who analyzed the cyclic operation of the Tajoura seawater reverse osmosis plant in Libya designed to produce 10 000 m^3/day. Slow construction of conveyance works meant that only 50% of the RO modules in the plant were used and then only for periods long enough to fill the freshwater storage reservoir. The result was 149 days of operation out of 379 days, operational periods ranged from 0.333 to 18 days and shutdown periods from 1-30 days. It should be noted, however, that this was a conventionally powered system performing under constant conditions while it was operating. Abufayed observed no abnormal variations in membrane performance over this time and attributed the slow rise in salt flux across the membranes during the period to natural membrane deterioration also observed in continuous flow mode systems.

A study by de la Nuez Pestana et al (2004) includes as an objective, the study of membrane behaviour under fluctuating operation. Operation of the plant was described as occurring for periods during 2001 and 2003 with a total run time of 7000 hours with the statement made by the authors that reverse osmosis membranes allow for variable functioning without deterioration, although additional information is needed on aging. Unfortunately no useful data is presented in the article on membrane performance over time to back up this claim. Similarly experiments were carried out by Gocht and Sommerfeld (1998) to prove the technical feasibility of transiently operating RO; transmembrane pressure was increased linearly (up to 180 bar/min) and step-wise (from 10 to 60 bar) with salt rejection and permeate flux measured as a function of time. No data from these experiments was reported; however, the authors made the comment that nothing was observed to rule out the transient operation of RO.

Rabinovitch (2008) in her thesis work described in more detail the performance of the system described by Heijman et al. (2009) and found that poor permeate quality was caused by damage to one of the membranes causing leakage. It is possible that this damage was caused by the fluctuating operation of the system.

Objective:

The objective of this research was to determine if a reverse osmosis membrane, exposed to fluctuating operation, would operate for an extended period of time without deterioration in performance. Performance will be evaluated by the membrane permeability coefficient, K and salt rejection, R. Results from these experiments will determine the suitability of the RO membrane to be directly coupled to a RES.

2. MATERIALS AND METHODS:

2.1 Description

The reverse osmosis unit used in this experiment is a Spectra™ LB 1800. This unit is a commercially available reverse osmosis desalination unit designed for land-based applications. Details of this unit are provided in Table 1 with a picture of the assembled experimental apparatus in Figure 1.

Table 1: Details of Spectra LB 1800

Power supply	Max. 30 Volt, 30 amps (900W)
Membranes	Two Filmtec 4x40 inch SW30 40-40 saltwater thin-film composite spiral-wound membranes.
Energy recovery	Spectra Pearson Pump
Capacity	Maximum rated production of 7.9 m^3/day

Figure 1: The experimental set-up (computer and control devices behind wooden frame)

The Spectra unit was assembled as per the manufacturer's instructions; this is a quick and simple process since most components come pre-assembled. A Liquiflo™ 37R positive displacement magnetic-drive pump was used as a feed pump for the high pressure Pearson pump, with a pressure relief valve between the two pumps to prevent over-pressurizing this line. The feed water source was a 1 m^3 reservoir of artificial seawater made up at 32 800 mg/L NaCl with tap water to emulate the osmotic pressure of seawater. The conductivity of the artificial seawater was measured then calibrated in dilutions to determine the relationship between conductivity and concentration. This gave the formula:

(1) $y = 0.65 * x$ where y = concentration (g/L NaCl)
x = conductivity (mS/cm)

Using this equation the conductivity of the reservoir water will be maintained at:

$x = 32.8 / 0.65$

$y = 50.5$ mS/cm

Feed water was delivered at 1 bar by the feed pump through a 5 micron cartridge filter. Pressure of the feed water could be monitored via the analogue pressure gauge at the inlet of the 5 micron filter. Pretreatment of feed water can have a significant impact on membrane performance (Choi et al., 2009), however in this experiment the use of high quality, re-circulated feed water made this influence negligible.

The feed water then passed through an analogue flow meter before entering the Pearson pump. A continuously computer monitored pressure gauge was located on the high pressure outlet of the Pearson pump. The high pressure salt water passed through both the FilmTec SW30 40-40 RO membranes in series where the stream was separated into a brine and permeate stream. The high pressure brine stream passed back through the Pearson pump for energy recovery before discharging back into the reservoir. The permeate stream passed through a continuously computer monitored flow transducer then conductivity transducer before passing through the provided analogue flow meter and back to the reservoir. In this way the system is closed with the artificial seawater being withdrawn, separated, then mixed back in to the reservoir. Both the permeate and the brine discharge lines were connected to a 'T' joiner before entering the reservoir to ensure proper mixing.

Operation of the system was controlled via the Dasylab computer program. A variable voltage was connected to the speed control pot of the Pearson high pressure pump (HPP); through this an input of fluctuating voltages can be used to operate the system as it would if powered by a RES. For this experiment, one week of 1-minute average wind speed data was obtained from the Hatenboer-Water 'Drinking with the Wind' project at a site in Schiedam, Netherlands. The period from 31/08/2009 to 6/09/2009 was chosen as it had a good distribution of high and low wind velocities. Figure 2 shows the trends for this period using data averages from 15 minute intervals; however, for the simulation, 1 minute data was used such that the speed of the pump is adjusted every minute (when there is fluctuation in the data). A similar system was used to control the speed of the feed pump to match the fluctuating speed (and thus consumption) of the HPP. The Dasylab program logs data for membrane pressure, permeate flow and permeate conductivity every second which can then be analyzed and graphed through the 'Matlab' program.

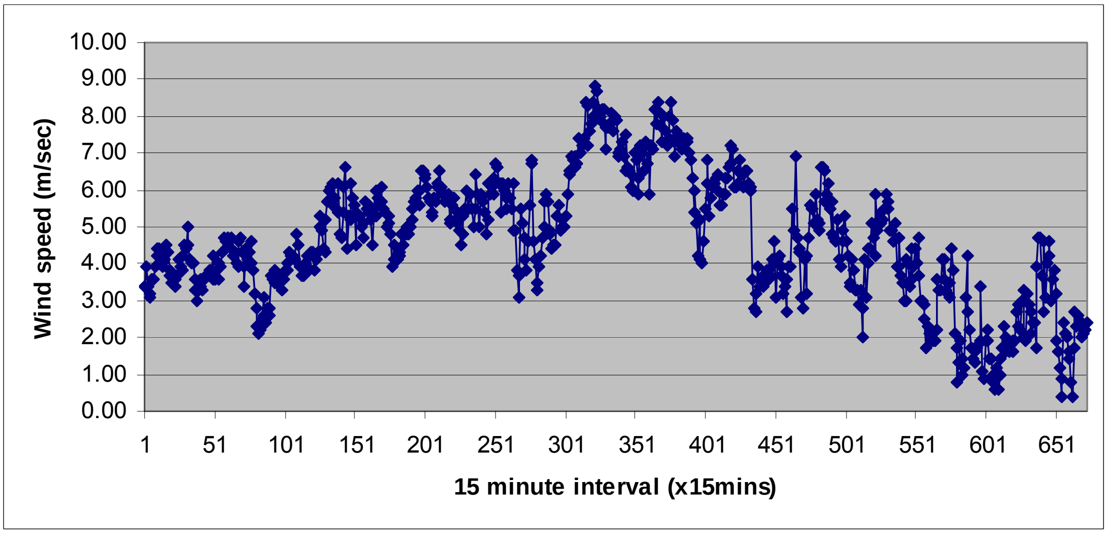

Figure 2: Wind speed distribution over 1 week at Hatenboer-Water site, Schiedam, Netherlands.

Prior to commencement of the simulations, the membranes were tested using demineralized water (DW) to determine the membrane permeability coefficient. The control panel of the LB 1800 contained a 3-way valve that can shift between a normal 'RUN' cycle, where feed water enters through the line connected to the pre-filter, or 'FLUSH' cycle, where suitable water for freshwater flushing of the membranes could enter the system via a separate line. This separate line was run to the second storey above where the experimental unit was positioned to an 80 litre tank containing DW. Once a siphon is created, this water can be gravity fed to the HPP for flushing of the membranes. The flush ratio can be determined by:

(2) $F = V_f – V_c / V_m$

where F = flush ratio
V_f = volume used for flush (L)
V_c = volume of water retained in the Spectra LB 1800 when it is dormant (L)
V_m = volume of water in membranes (L)

Once the experiment was running, the unit was stopped during a period of low speed and fresh water flushed. This would be similar to a unit set up in the field that stops production when wind power is not adequate and flushes the membranes with fresh water to reduce biofouling and maintain product water quality. The membranes were flushed with one 80L tank of DW to remove salts and then a second to recalculate the membrane resistance coefficient to monitor if this value changes with operating time. The flushing ratio of the membranes during each DW flush was then calculated as:

Using equation (2)

(2) $F = V_f – V_c / V_m$
$= (180 – 16) / 15$
$= 9.6$

Therefore the water was exchanged 9.6 times through the reverse osmosis membranes during each flush cycle stoppage. A calculation of the membrane permeability coefficient was performed for each freshwater flush using the average product water flow and membrane inlet pressure from the last 100 seconds of the DW water flush. The final 100 seconds was chosen as the averaged period as it is assumed that the flush has had maximum effect of rinsing the membranes by this stage and the measured parameters have steadied.

The rejection of salts were then calculated using the formula

(3) $R = 1 - (c_p/c_f)$ Where R = rejection
c_p = concentration in permeate (g/m^3)
c_f = concentration in feed (g/m^3)

Figures for rejection can be calculated during short periods of steady operation in between the fluctuating operation cycles. During these periods the speed of the system was adjusted manually in 0.5V increments and all measurable parameters recorded once stabilized.

In order to maintain the concentration of the artificial seawater at a constant level during the DW flush the initial concentrate discharge was directed into a bucket to capture the salts being flushed out. Once the conductivity of this discharge water approaches 50.5 mS/cm the remainder was directed to waste with the captured water being returned to the reservoir. Similarly once the flush had been completed and the system put back into a regular cycle, the initial discharge water was discarded until the fresh water had been flushed from the system. Further adjustments to the level and conductivity of the reservoir water were made as necessary to ensure constant characteristics.

2.2 Setting the operating range

Prior to acquiring a feed pump to deliver the salt water, some tests were conducted to determine the operating range of the HPP with mains pressure tap water. Spectra, the manufacturers of the LB 1800 RO unit used in this study, recommend that feed flows greater than 19 L/min are implemented to maintain sufficient cross-flow velocity to minimize scaling. Due to the low levels of hardness in the Delft tap water (<1.5 mmol/L, www.evides.nl) used to prepare the artificial seawater, this was not perceived to be a problem. Rather as lower speed as practical was discovered in order to have the greatest range of fluctuation available to test the RO membranes. A test was performed, reducing the speed of the HPP until audible unstable operation of the pump was observed. This limit was found to be a speed voltage of 6V and was set as the lower limit. The upper limit of the range was found to be restricted by the output of the power inverter used for the experiment. During the initial testing this was 9.7V so was close to the limit of the system, as the computer has a maximum output of 10V. At the low speeds used the motor of the HPP appeared to have inadequate cooling, so an external fan was used to control motor temperature.

3. RESULTS AND DISCUSSION

3.1 Description of Tests

Initial membrane permeability coefficient

Four separate tests were run to determine the membrane permeability coefficient once the preservative had been flushed from the membranes using tap water (non-chlorinated in the Netherlands). Each test consisted of running the system in the flush cycle using 80 L DW until the tank was emptied. Results are presented in table 2 with the mean of the tests being used to calculate the membrane permeability coefficient.

Table 2: Membrane pressure and permeate flow during initial DW tests

Test number	Membrane Pressure (bar)	Permeate Flow (L/min)
1	7.06	4.04
2	6.79	3.98
3	6.94	4.04
Mean	**6.93**	**4.02**

Equation 3 represents the flow of permeate through the membrane.

(3) $Q = K/\mu * A * (\Delta P - \Delta\pi)$ where
Q = permeate flow (m^3/s)
K = membrane permeability coefficient (m)
μ = viscosity of water (Pa/m^2)
A = area of membrane (m^3)
ΔP = membrane pressure inlet – membrane pressure outlet (Pa)
$\Delta\pi$ = osmotic pressure in membrane (Pa)

If we assume that the pressure drop through the pressure vessel and the osmotic pressure of DW is negligible, then ($\Delta P - \Delta\pi$) can be expressed as the membrane inlet pressure (P_{inlet}). Therefore rearranging equation 3;

(4) $K = (Q * \mu) / (A * P_{inlet})$

$K = (6.7*10^{-5}\ m^3/s * 1.0*10^{-3}) / (15.8\ m^2 * 6.93*10^5\ Pa)$

$K = 6.11*10^{-15}$ m

Production tests

These tests were run continuously for various lengths of time using artificial seawater and fluctuating operation. An example of a production period can be seen in figures 3(a) and 3(b).

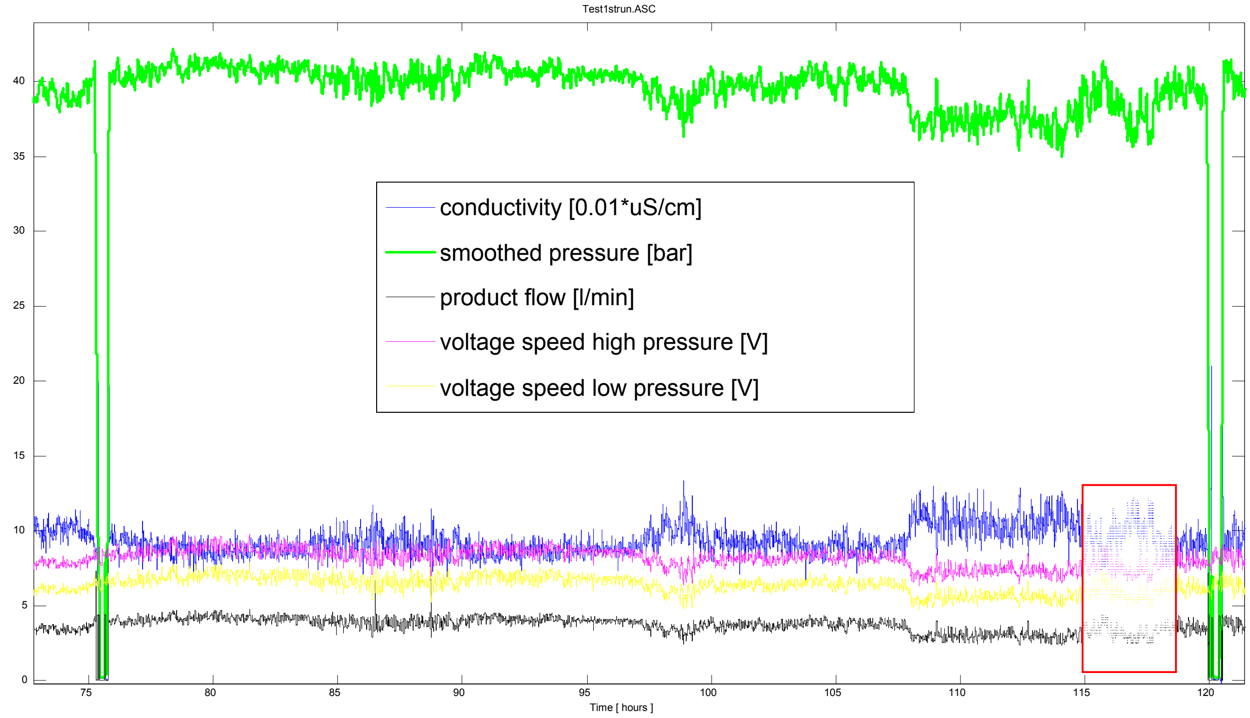

Figure 3(a): A period of operation over 2 days during test 1.

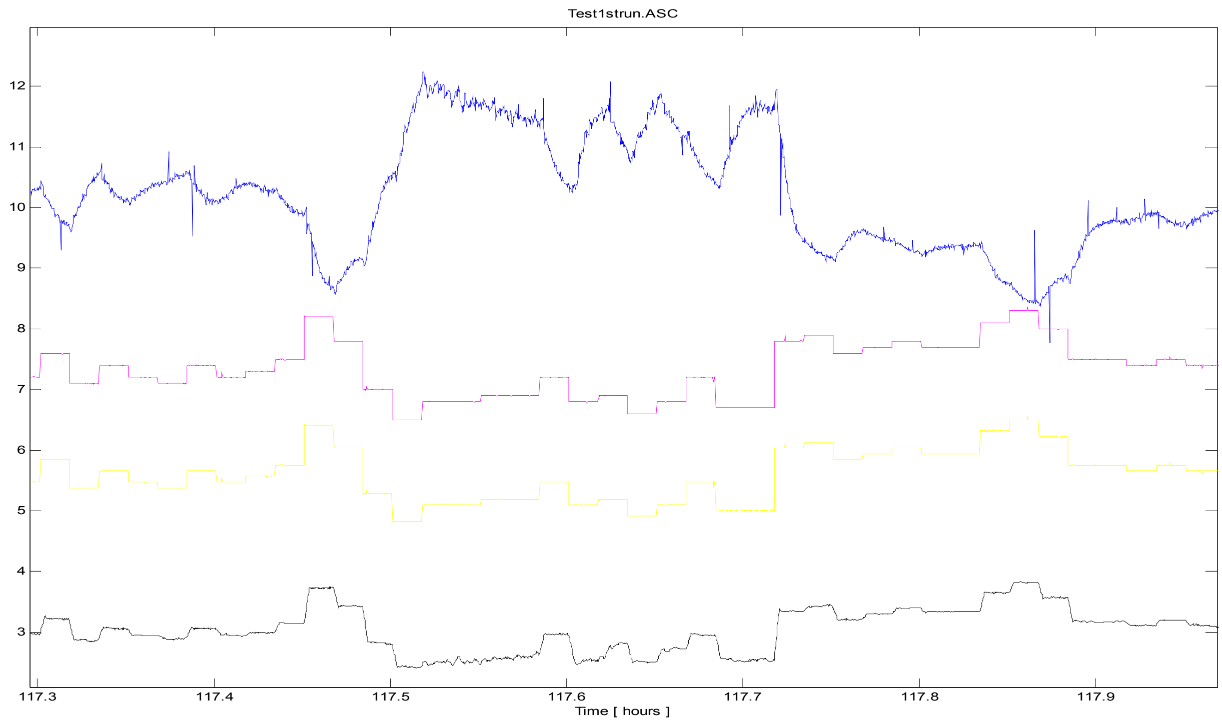

Figure 3(b): A magnified view of a section from figure 3(a)

It can be observed in *figure 3(b)* the changes in speed of the HPP (purple line, V) every minute where there was a change in the corresponding raw wind data. The speed of the low pressure pump (yellow line, V) runs in parallel with the HPP via the computer program to maintain constant feed pressure to the HPP. The permeate production (black line, L/min) responds almost proportionally to the change in speed of the HPP since the Pearson Pump is a 20% recovery fixed displacement pump, meaning for 100% of feed water that enters the pump approximately 80% of the concentrate is used in the energy recovery system with the remaining 20% permeate production. Therefore at higher speeds, the flow through the pump is increased and permeate production also increased.

The conductivity of the permeate (blue line, *0.01 µS/cm) responds inversely to the production of permeate, since the diffusion of salts across the membrane is constant if the concentration in the feed water is constant, as shown in the equation

(5) $Qs = K_2 * A * C_f * 2 - \gamma / 2(1 - \gamma)$

Where Qs = salt flux (g/s)
K_2 = membrane salt permeability (m/s)
A = area membrane (m^2)
C_f = concentration in feed (g/m^3)
γ = recovery
All of which should remain constant in this experiment.

Therefore a higher permeate production will lead to a greater dilution of the diffused salts in the permeate and lower the conductivity. Conversely when the HPP is running at low speeds and producing low volumes of permeate, the conductivity will increase. It can be seen in *figure 3(a)* that the trend of pressure (green line) follows that of permeate production which relates to the relationship expressed previously in equation (3) where an increase in ΔP causes an increase in Q.

Table 3: Summary of Tests

				AVERAGE			
TEST	**OPERATION TIME (hrs)**	**SPEED V RANGE (av.)**	**EQUIVALENT RPM (av.)**	**PROD (m3/day)**	**PRESS (bar)**	**TDS (mg/L)**	**kWh/m3**
1	120.8	6-9,7 (7,83)	499-964 (729)	5.03	39.36	638	2.66
2	94.2	6-9,7 (7,84)	499-964 (730)	5.03	39.62	609	2.67
3	19.8	6,5-8,2 (7,39)	562-776 (674)	4.5	38.47	643	2.67
4	2.1	revised operation of system					
5	64.9	7,6-9,3 (8,39)	700-914 (800)	5.33	39.6	523	2.84
6	21.9	7,8-8,7 (8,25)	725-839 (782)	5.29	40.72	518	2.78
7	141.8	7,7-10 (8.8)	713-1002 (851)	5.82	41.79	519	2.82
7b	138.5	7,7-10 (8.87)	713-1002 (860)	5.83	42.21	518	2.86

A full description of the tests is given in appendix 1. A summary of all the tests is presented in table 3. Various adjustments were made to the system during the course of the testing to improve the smoothness and efficiency of the system, such that it could be applied to long term operation in the field. It also became important once the operation of the system was stabilized in a fluctuating pattern, that the average TDS of the permeate during periods of operation be within drinking water standards. The drinking water standard established by the World Health Organization (WHO) sets a limit of 500 mg/L TDS. It can be seen in table 3 that none of the tests over an extended period of time had averages below the target of 500 mg/L.

It was observed on day 5 of test 1, during the last flush, that a thin, fibrous material which appeared to be fragments of a biofilm, was discharged from the concentrate line. This observation was repeated at the end of nearly all of the subsequent DW flushes and fragments were also found on the 5µm pre-filter when it was removed during a shutdown period.

An attempt was made to replicate Test 7 to check the consistency of results (Test 7b). Unfortunately a power failure caused a premature stoppage and prevented an exact replication of the test; however the test results show a difference within the 2% error range of the instrumentation suggesting consistent data.

3.2 Establishing relationships and trends

During stoppages in the testing cycles, it was often necessary to run trials under controlled conditions to establish and confirm relationships between one or more variables. Relationships not directly related to the objectives of the experiment are dealt with in Appendix B, those relating to the objective are outlined here:

Temperature

Since there was no heat exchanger in the system to control the temperature of the reservoir water, it was necessary to monitor the temperature to establish what effect (if any) it would have. The temperature was monitored via the conductivity meter for the permeate at random intervals over two continuous periods of operation. The results are presented in Figure 4.

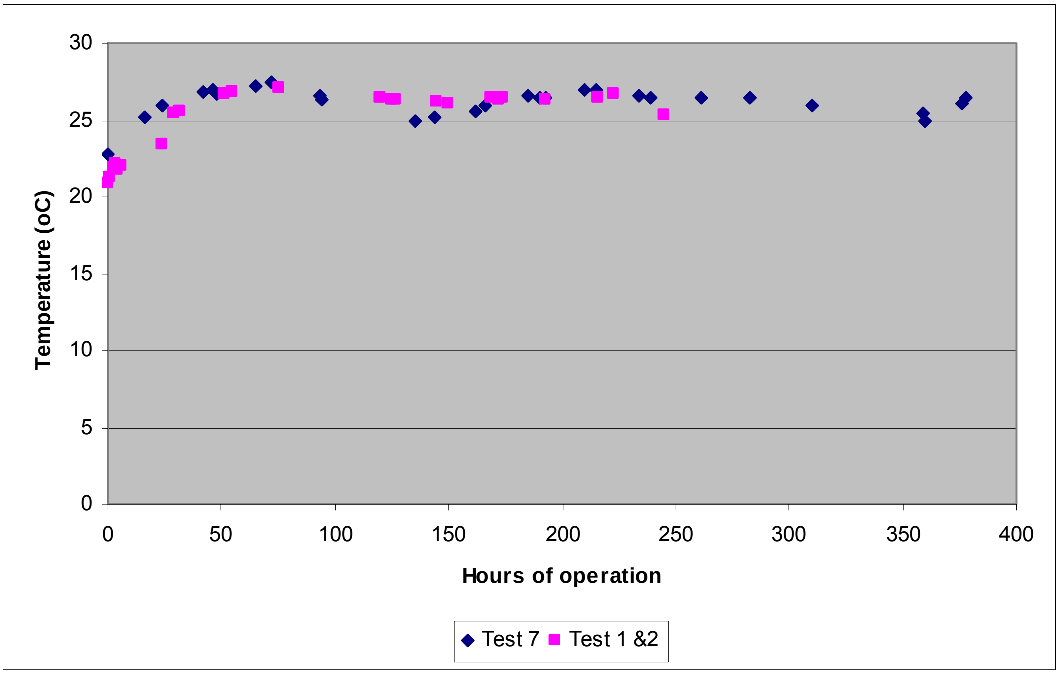

Figure 4: Establishing trends in temperature of reservoir water.

The importance of water temperature relates to determination of the K-value; if there are large fluctuations then this will need to be compensated for in the parameters of equation 4. As demonstrated in Figure 5 the temperature of the recirculated water rises steadily during the first

24 hours, then stabilizes at 26°C +/- 1°C. Slight fluctuations result from the intensity of operation of the system as well as a slight decrease in temperature of the laboratory over the weekend when the heating system is turned down (evident where there are gaps in the data points since there was no access to the laboratory on Sunday).

Membrane Permeability Coefficient, K

The membrane permeability coefficient, K, was determined during the DW flush to provide controlled conditions for calculations in between periods of fluctuating operation. As a further indication of the effects on membrane performance after periods of fluctuating operation, the value of K was also determined using average figures for product flow and pressure during operation periods between the DW flushes. Results are represented in figure 5.

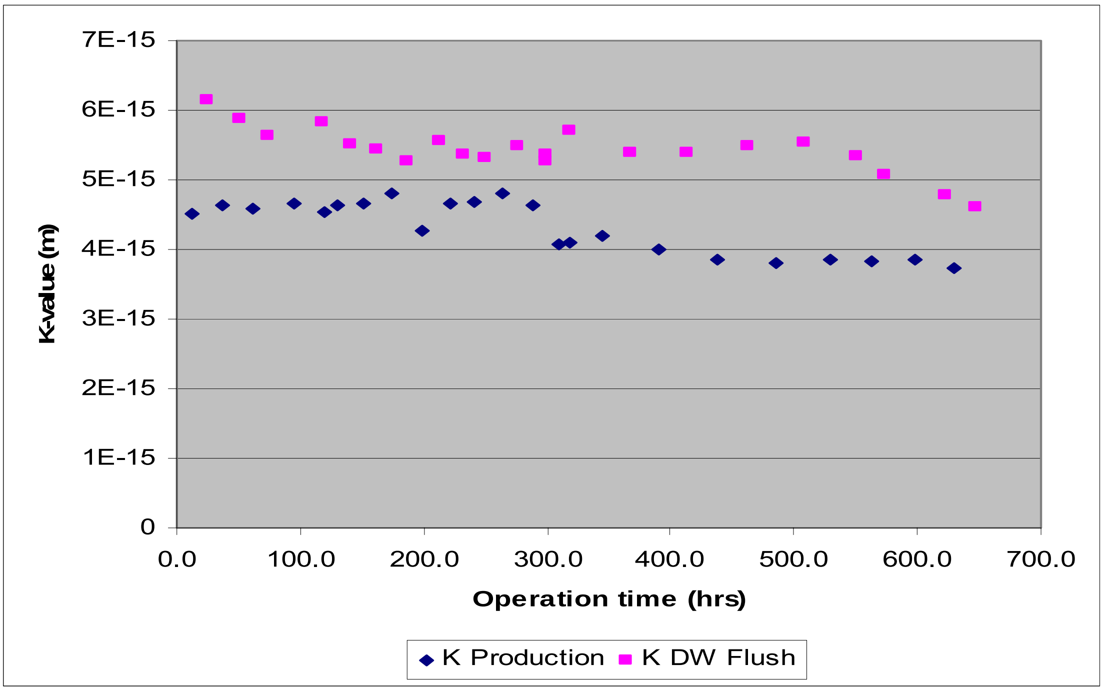

Figure 5: Trends in the membrane permeability coefficient, K

The first thing that is noticed in figure 5 is that the values of the production K-value and the DW flush K-value are significantly different. In theory the membrane permeability coefficient should be constant at a specific point in time regardless of the conductivity of the water passing through it, providing there is an accurate estimation of flux, transmembrane pressure (TMP) and the dynamic viscosity of water.

This difference is likely the result of concentration polarization, the phenomenon whereby salt ions accumulate in a layer on the surface of the membrane, increasing the osmotic pressure at the membrane surface. The process is described in more detail during an extensive description of the reverse osmosis process by Fritzmann and authors (2007). The rate of concentration polarization occurring in these experiments is difficult to predict during fluctuating operation. The process is reversible in the absence of precipitating substances such as $CaCO_3$ and $CaSO_4$ as is the case in this experimental system. Therefore when only considering salt accumulation concentration polarization is more pronounced during periods of low pump speed and low permeate flux. However at the highest speeds, with increased cross-flow velocity and flux concentration, it is expected to have a minimal effect.

An estimation of concentration polarization can be made if the average DW K-value is assumed for the membrane during production. From equation 3:

$$Q_{av.\ prod} = K_{av.\ DW} / \mu * A * (\Delta P_{av.prod} - \Delta\pi)$$
$$6.22*10^{-5} = 5.47*10^{-15} / 0.88*10^{-3} * 14.8 * (40.5*10^{5} - \Delta\pi)$$
$$\Delta\pi = 33.7 * 10^{5}\ \text{Pa}$$

If the osmotic pressure of the permeate is assumed to be negligible then the osmotic pressure is approximately that at the membrane surface.

$$\Delta\pi \sim \pi_m$$

Concentration polarization is calculated as:

$$\beta = \pi_m / \pi_f$$
$$\beta = 33.7 * 10^{5} / 27.9 * 10^{5}$$
$$\beta = 1.2$$

Thus the concentration of salts at the membrane surface is approximately 1.2x the concentration in the feed water. An underestimation of osmotic pressure when calculating the membrane permeability coefficient can lead to an overestimation of the K-value and may explain the difference in figure 6.

The most important point to be obtained from figure 6 in relation to this study is that the trends do not evolve in a positive direction (upward trend) as this would indicate damage to the membrane over time caused by the fluctuating operation. Instead, both the production and DW flush K-value figures show a slightly negative trend. This is a trend generally common to all reverse osmosis systems due to fouling and compression of the membrane (Fritzmann et al, 2007). In this case the observation of small pieces of biofilm being ejected during DW flushes would suggest some mild biofouling is occurring in the membranes. A further explanation could be a change in the characteristics of the membrane due to compression of the membrane once production under high pressure (full strength sea water) had commenced.

Rejection of Salts

Values for rejection of salts were calculated during periods of controlled system testing during Tests 4 and 7. The results presented in figure 6 show no significant difference in salt rejection between the two tests.

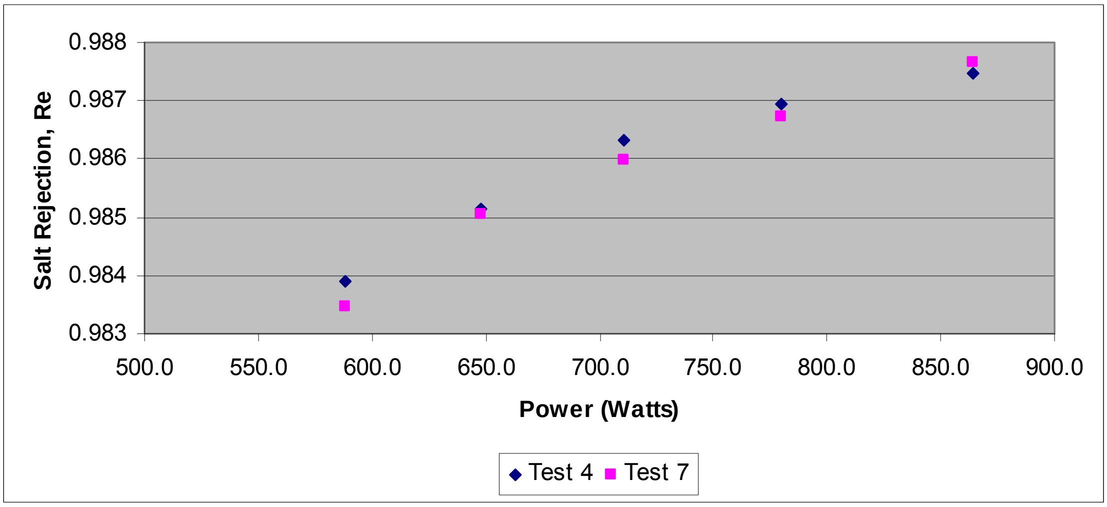

Figure 6: Comparison salt rejection

3.3 Implications of findings

Given that the results obtained thus far suggest no rising trend in the membrane permeability coefficient and no change in salt rejection, it can be concluded that fluctuating operation does not affect membrane performance, at least for the first 650 hours of operation. This then satisfies the objective and gives promise for the further development of technology directly coupling renewable energy to reverse osmosis.

The focus of the analysis then moved to the production and quality of the permeate produced by the experimental set-up and how this can be translated to use in the field. It can be noted in Table 3 that the tests generally achieved lower average values for TDS as the average speed of the HPP progressively increased. Despite this, even the last tests shown do not achieve an average TDS below the WHO guideline limit of 500 mg/L (minimum test 6 and 7b of 518 mg/L).

Interesting results from test 7 can be found in the sub-set of data from days 2/3 and 4/5 of the production cycle (Table 4). It can be seen from this table that two separate sets of wind speed data are used, both tests run for approximately the same time and have the same average HPP voltage speed, production and pressure for the operation period. What is significantly different is the average TDS. Test 7 (2/3) achieves a TDS below the guideline of 500 mg/L while Test 7 (4/5) is significantly higher.

Table 4: Example of difference in Test 7 from days 2&3, 4&5

TEST	HOURS	Av. HPP SPEED (V)	Av. PRODUCTION (m3/day)	Av. PRESSURE (bar)	Av. TDS (mg/L)
7 day 2/3	47	8.9	5.9	42	495
7 day 4/5	45	8.9	5.9	42	535

Previously table 3 showed that Test 7 was replicated (Test 7b) to ensure consistency of results so we can assume that the difference in the TDS is not due to error in the measurements. A possible explanation could relate to the relationship between TDS and product flow to the power fed to the HPP (Figure 7).

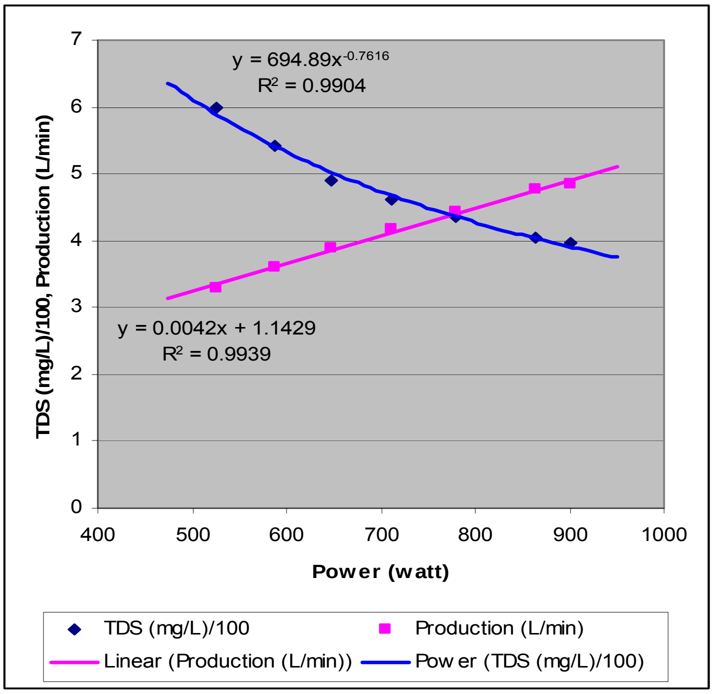

Figure 7: Relationship between TDS and product flow to power fed to HPP
(Displayed are the coefficients of determination for both trends as well as the linear function for the Product flow relationship (top) and the power function for the TDS relationship (bottom) with Power. Data points taken from trials conducted prior to the start of Test 7)

Figure 7 shows a power function relationship between TDS and Power of the HPP. This is primarily due to the constant flux of salt across the membrane compared to the varying flux of water with pressure. This may be explained by the solution diffusion model (SDM) that is based on the following assumptions:

- Permeating components dissolve into the membrane phase.
- There is at all times an equilibrium at the phase interface between membrane and feed/permeate side.
- Salt and water flux are independent of each other.
- Salt flux is independent of pressure and results solely from concentration gradient.
- The membrane permeability coefficient and water concentration across the membrane is constant.

While this last assumption could be argued, given the results from these experiments, the change in the membrane permeability coefficient between Test 7, days 2/3 and 4/5, can be assumed to be negligible. This means that the diffusion of salt across the reverse osmosis membrane will increase as the concentration on the membrane surface increases. Figure 7 also illustrates a linear relationship between the permeate production and RPM of the HPP. This is primarily due to the increase in TMP (refer to equation 3) resulting from increased speed of the HPP.

These two trends in Figure 7 are related, since at high power (and thus RPM) there is a high cross-flow velocity through the membranes disturbing any potential concentration polarization, coupled with a high dilution of the salts diffusing through the membrane, due to the high production of permeate. Alternatively, at low power the cross-flow velocities and permeate production are low, leading to a potential increase in concentration polarization and low dilution of the diffused salts on the permeate side.

It is suggested then that the operational cycle of production can have a significant influence on the average permeate TDS over an extended period of time. Consider the following examples (Figure 8):

(a)

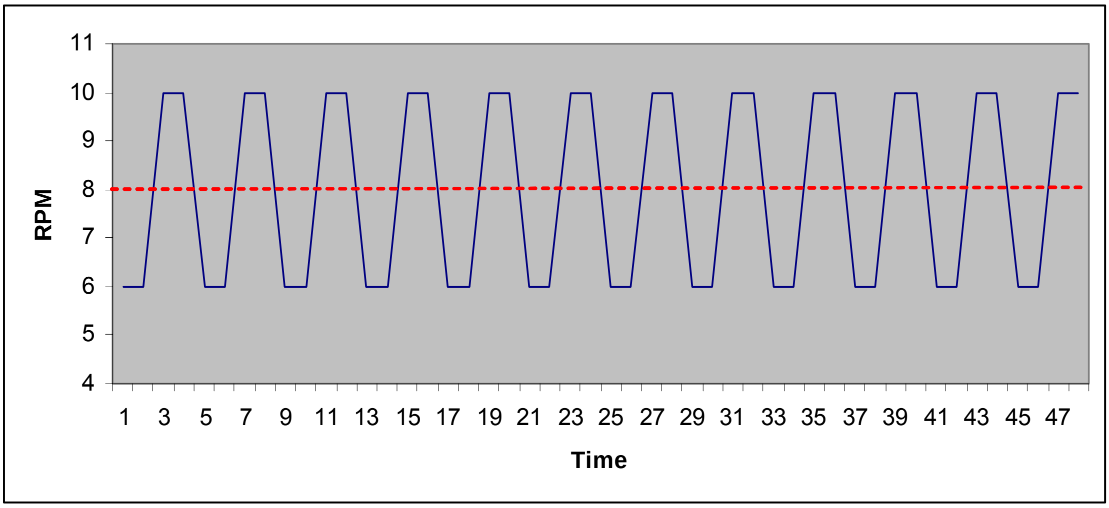

(b)

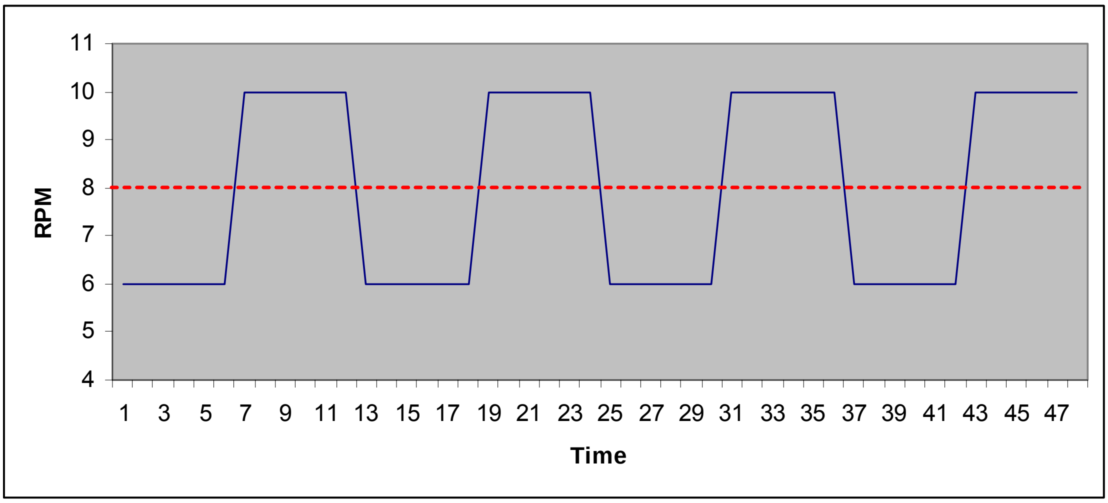

Figure 8 (a) and (b): Examples of operational cycles with the same mean speed of HPP

These two examples represent simplified detail of different wind speed patterns assuming a directly coupled system and a linear relationship between wind speed and RPM of the HPP. Figure 8 (a) represents gusty conditions with short periods of high and low wind speeds. In Figure 8 (b) the periods of high and low are for longer periods. Both periods of operation share the same minimum and maximum range and the same mean speed of operation.

If we now relate this back to salt flux and the SDM, we can expect that in Figure 8 (a), with its short periods of low HPP speed followed by sharp increases, that the effects of concentration polarization will be quickly dissipated and have little effect on long term permeate quality. On the other hand, in Figure 8 (b) during sustained periods of low speed operation, the effects of concentration polarization and increased TDS of the permeate are likely to be more significant and contribute to a higher average TDS over long term operation. This is an important consideration for engineers when designing such systems to consistently achieve a water quality target below 500 mg/L TDS. Kiranoudis et al. (1997) mentions the need to oversize components when designing site specific wind/RO plants; however, their reasoning is based more on achieving target production with fluctuating wind conditions rather than target quality.

An attempt was made to reproduce this effect using artificial data similar to that shown in Figure 8 for run times of 4 hours with periods of high speed for 1 minute then low speed for 1 minute, recurring. This was then repeated with 4 minutes high speed then 4 minutes low speed, recurring and lastly with 8 minute periods recurring. The results presented in Table 5 were inconclusive and longer periods may be needed to achieve the predicted results. Unfortunately there was no time for further trials; however, it would make for interesting further research.

Table 5: Controlled periods of fluctuating operation

PERIOD (min)	RUN TIME (hr)	AVERAGE TDS (mg/L)
1	4	528.5
4	4	533
8	4	529.1

3.4 Trials with new membrane

At the beginning of the trials with artificial seawater, the conductivity of the separate membranes was tested. For a two stage system such as the one used in the experiments, it is expected that the second membrane permeate will have a higher conductivity than the first, since its feed is the higher salinity brine from the first membrane with subsequently higher osmotic pressure. The difference was found to be substantial between the two membranes; 673 µS/cm for the first compared to 1589 µS/cm for the second. This equates to salt rejections of 0.987 and 0.972 respectively. It appears then that we had one slightly loose membrane as the manufacturer suggests a rejection of 0.98. In the interests of the original objective of testing the effects of fluctuating operation on reverse osmosis membranes, it seemed advantageous to test membranes with slightly different characteristics.

After it became evident that fluctuating operation was not causing detrimental effects to either membrane over the period of operation, the focus turned to applications of the unit. It was decided that the second membrane should be replaced to determine whether this had any effect on overall permeate quality. Another FilmTec® SW30 40-40 membrane was purchased and installed and preliminary tests showed significant improvement: 610 µS/cm for the first membrane and 948 µS/cm for the new second membrane, salt rejections of 0.988 and 0.983 respectively. This has the advantage of giving a greater operation range for the Spectra reverse osmosis unit.

3.5 Practical applications of the research

An article will be produced from this research to contribute to the body of knowledge in the public domain regarding the effects of fluctuating operation on reverse osmosis membrane performance. Data from this study will be used to conduct further experiments with the test rig and trial its coupling with photovoltaic energy in TU Delfts' *Drinking with the Sun* project. Data will also be used in the continuing *Drinking with the Wind* Project.

Practical Example:

A stand alone reverse osmosis desalination system directly coupled electrically (no batteries) to a wind turbine is considered. For the Spectra unit described in this report, it may be beneficial to use two units to increase the range of operation and achieve greater production. In this way, as wind speed increases from calm conditions, one unit can start operation once power is available and if wind speed continues to increase, the second unit can also come into operation. The main advantages of the Spectra LB 1800 are

a) 'out-of-the-box' assembly: the unit comes mainly pre-assembled so time and cost to set it up on site is minimal.
b) Very efficient: as shown in Table 3 the average power consumption of the unit is less than 2.9 kWh/m^3.

A 5 kW wind turbine would be suitable for this application; these turbines can be purchased in a compact kit form for transport and easily assembled on site. With tilt-up support poles there is no need for cranes to erect them. A suitable site for utilization of wind power will ideally have an average wind speed of over 7 m/s. At this wind speed a 5 kW turbine such as the Fortis Wind Energy 'Montana' wind turbine will produce around 1.1 kWh (Fortis Wind Energy website).

An estimation of cost (€) could then be made:

RO units x2 (@13 000 each)	26 000
5 kW wind turbine	18 000
Feed pump and tanks	6 000
Assembly and automation	10 000
Overall Capital cost	60 000

Depreciated over 10 years plus maintenance (including replacement RO membranes and pre-filters, etc) of 2 000 per year

60 000 / 10 = 6 000; 6 000 + 2 000 = € 8 000 / year water cost

Production of water = (1.1kWh * 24 * 365) / 2.9 kWh/m^3 = 3 323 m^3/year

Production cost of water = 8 000 / 3 323 = **€ 2.4 / m^3**

Although this price is higher than mains delivered water (approximately €1.50 in the Netherlands) it is likely to be much cheaper than transporting water or diesel for a generator to the remote locations this technology is targeted at and compares favourably with prices quoted in the Introduction.

4. CONCLUSIONS

During over 650 hours of fluctuating operation, the DOW FilmTec SW30 40-40 reverse osmosis membranes showed no leakages. A slight deterioration in performance was attributed to biofouling. In practice, fluctuations in wind speed would be unlikely to translate as quickly into changes in HPP speed as they were for these tests, due to the smoothing effect of the inertia of the wind turbine. It can be suggested that these tests represent a 'worst case' fluctuation in operation for the RO membranes, giving confidence that they will perform appropriately when applied in the field. There is still a lack of long-term data on the fluctuating operation of RO membranes that this research has not fully satisfied and further investigation would be very useful.

Many of the problems encountered with maintaining stable operation during the first tests can be attributed mainly to feed pressure and perhaps, to a lesser extent, to the seating of the valves in the new pump. It became apparent that there was a narrow range of feed pressures that resulted in smooth operation throughout the speed range of the HPP. These sorts of difficulties are to be expected in a system that is not designed for fluctuating operation but rather operation at a stable speed. Perhaps there is a need for research into pumps and energy recovery systems designed especially for fluctuating operation if directly coupled systems are to be optimized.

The trials conducted also suggest that the pattern of fluctuating operation can have an impact on the quality of the permeate produced. This is important if designing a system to consistently produce water below the WHO guideline; however, it is important to remember that this is only an aesthetic guideline rather than a health related one, and in practice an isolated community will be grateful for a consistent quantity of water and is unlikely to be concerned if the quality rises slightly over 500 mg/L TDS periodically.

Lastly it is noted that the performance of individual membranes can vary significantly, even the same model membrane from the same manufacturer. This can also have an effect on the quality of permeate produced and the potential operating range of the RO system. It would be prudent perhaps to test the individual membranes of a system where practical to ensure they perform as expected before commissioning of the system.

Directly coupled RES/RO desalination systems do have the potential to improve the lives of many people in remote and isolated communities lacking appropriate infrastructure and potable water. This research has taken another small step towards proving this technology, however there is still much work to be done to improve the reliability and efficiency to make systems robust and affordable for widespread implementation.

5. REFERENCES:

Abdel-Jawad, M., El-Sayed, E.E.F., Ebrahim, S., Al-Saffar, A., Safar, M., Tabtabaei, M. and Al-Nuwaibit, G. (2001), 'Fifteen years of R&D program in seawater desalination at KISR Part 2. RO system performance', *Desalination*, 135, 155-167.

Abufayed, A.A. (2003), 'Performance characteristics of a cyclically operated seawater desalination plant in Tajoura, Libya', *Desalination*, 156, 59-65.

Ahmad, G.E. and Schmid, J. (2002), 'Feasibility study of brackish water desalination in the Egyptian deserts and rural regions using PV systems', *Energy Conservation and Management*, 43, 2641-2649.

Ahmed Shata, A.S. and Hanitsch, R. (2008), 'Electricity generation and wind potential assessment at Hurghada, Egypt', *Renewable Energy*, 33, 141-148.

Alawaji, S., Smiai, M.S. and Rafique, S. (1995), 'PV-powered water pumping and desalination plant for remote areas in Saudi Arabia', *Applied Energy*, 52, 283-289.

Al-Bastaki, N.M. and Abbas, A. (1999), 'Improving the permeate flux by unsteady operation of a RO desalination unit', *Desalination*, 123, 173-176.

Al-Bastiki, N.M. and Abbas, A. (1998), 'Periodic Operation of a Reverse Osmosis Water Desalination Unit', *Separation Science and Technology*, 33:16, 2531-2540.

Alexiadis, A., Bao, J., Fletcher, D.F., Wiley, D.E. and Clements, D.J. (2006), 'Dynamic response of a high-pressure reverse osmosis membrane simulation to time dependent disturbances', *Desalination*, 191, 397-403.

Al Suileimani, Z. and Nair, R. (2000), 'Desalination by solar-powered reverse osmosis in a remote area of the Sultanate of Oman', *Applied Energy*, 65, 367-380.

Carta, J.A., Gonzalez, J. and Subiela, V. (2003), 'Operational analysis of an innovative wind powered reverse osmosis system installed in the Canary Islands', *Solar Energy*, 75, 153-168.

Charcosset, C. (2009), 'A review of membrane processes and renewable energies for desalination', *Desalination*, 245, 214-231.

Choi, Y.H., Kwoen, J.H., Kim, D.I. and Lee, S. (2009), 'Evaluation of various pretreatment for particle and inorganic fouling control on performance of SWRO', *Desalination*, 247, 137-147.

De la Nuez Pestana, I., Lattorre, F.J.G., Espinoza, C.A. and Gotor, A.G. (2004), 'Optimization of RO desalination systems powered by renewable energies. Part 1: Wind energy', *Desalination*, 160, 293-299.

De Munari, A., Capao, D.P.S., Richards, B.S. and Schafer, A.I. (2009), 'Application of solar-powered desalination in a remote town in South Australia', *Desalination*, 248, 72-82.

Eltawil, M.A., Zhengming, Z. and Yuan, L. (2009), 'A review of energy technologies integrated with desalination systems', *Renewable and Sustainable Energy Reviews*, 13, 2245-2262.

Evides website, www.evides.nl

Folley, M., Penate Suarez, B. and Whittaker, T. (2008), 'An autonomous wave-powered desalination system', *Desalination*, 220, 412-421.

Fortis Wind Energy website, www.fortiswindenergy.com/products/wind-turbines/montana

Fritzmann, C., Lowenberg, J., Wintgens, T. and Melin, T. (2007), 'State-of-the-art of reverse osmosis desalination', *Desalination*, 216, 1-76.

Gilau, A.M. and Small, M.J. (2008), 'Designing cost-effective seawater reverse osmosis system under optimal energy options', *Renewable Energy*, 33, 617-630.

Gocht, W. and Sommerfeld, A. (1998), 'Decentralized desalination of brackish water by a directly coupled reverse-osmosis-photovoltaic system; a pilot plant study in Jordan', *Renewable Energy*, 14(1-4), 287-292.

Harrison, D.G., Ho, G.E. and Mathew, K. (1996), 'Desalination using renewable energy in Australia, *Renewable Energy*, 8, 509-513.

Heijman, S.G.J., Rabinovitch, E., Bos, F., Olthof, N. and van Dijk, J.C. (2009), 'Sustainable seawater desalination: Stand-alone small scale windmill and reverse osmosis system', *Desalination*, 248, 114-117.

Herold, D., Horstmann, V., Neskakis, A. and Plettner-Marliani, J. (1998), 'Small scale photovoltaic desalination for rural water supply-demonstration plant in Gran Canaria', *Renewable Energy*, 14 (1-4), 293-298.

Herold, D. and Neskakis, A. (2001), 'A small PV-driven reverse osmosis desalination plant on the island of Gran Canaria', *Desalination*, 137, 285-292.

Houcine, I., Benjemaa, F., Chahbani, M. and Maalej, M. (1999), 'Renewable energy sources for water desalting in Tunisia', *Desalination*, 125, 123-132.

Infield, D. (1997), 'Performance analysis of a small wind powered reverse osmosis plant', *Solar Energy*, 61, 415-421.

Kalogirou, S.A. (2005), 'Seawater desalination using renewable energy sources', *Progress in Energy and Combustion Science*, 31, 242-281.

Keefer, B.G., Hembree, R.D. and Schrack, F.C. (1985), 'Optimized matching of solar photovoltaic power with reverse osmosis desalination', *Desalination*, 54, 89-103.

Kiranoudis, C.T., Voros, N.G. and Maroulis, Z.B. (1997), 'Wind exploitation for reverse osmosis desalination plants', *Desalination*, 109, 195-209.

Lee, R-W., Glater, J., Cohen, Y., Martin, C., Kovac, K., Milobar, M.N. and Bartel, D.W. (2003), *Desalination*, 155, 109-120.

Lui, C.C.K., Xia, W. and Park, J.W. (2007), 'A wind-driven reverse osmosis system for aquaculture wastewater reuse and nutrient recovery', *Desalination*, 202, 24-30.

Liu, C.C.K., Park, J., Migita, R. and Qin, G. (2002), 'Experiments of a prototype wind-driven reverse osmosis desalination system with feedback control', *Desalination*, 150, 277-287.

Manolakos, D., Papadakis, G., Mohamed, E.S., Kyritsis, S. and Bouzianas, K. (2005), 'Design of an autonomous low-temperature solar Rankine cycle system for reverse osmosis desalination', *Desalination*, 183, 73-80.

Miranda, M.S. and Infield, D. (2002), 'A wind-powered seawater reverse-osmosis system without batteries', *Desalination*, 153, 9-16.

Mohamed, E. Sh., Papadakis, G., Mathioulakis, E. and Belessiotis, V. (2008), 'A direct coupled photovoltaic seawater reverse osmosis desalination system toward battery based systems – a technical and economical experimental comparative study', *Desalination*, 221, 17-22.

Mohamed, E.Sh., Papadakis, G., Mathioulakis, E. and Belessiotis, V. (2006), 'An experimental comparative study of the technical and economic performance of a small reverse osmosis desalination system equipped with a hydraulic energy recovery unit', *Desalination*, 194, 239-250.

Park, G.L., Schafer, A.I. and Richards, B.S. (2009), ' Potential of wind-powered renewable energy membrane systems for Ghana', *Desalination*, 248, 169-176.

Petersen, G., Fries, S., Mohn, J. and Muller, A. (1979), 'Wind and solar powered reverse osmosis desalination units; description of two demonstration projects', *Desalination*, 31, 501-509.

Rabinovitch, E. (2008), 'Drinking with the wind; small scale SWRO-installation mechanically driven by wind energy', TU Delft.

Richards, B.S., Capao, D.P.S., Schafer, A.I. (2008), 'Renewable Energy Powered Membrane Technology 2; The effect of energy fluctuations on the performance of a photovoltaic hybrid membrane system', *Environmental Science Technology*, 42, 4563-4569.

Schafer, A.I., Broeckmann, A. and Richards, B.S. (2007), 'Renewable Energy Powered Membrane Technology 1; development and characterization of a photovoltaic hybrid membrane system', *Environmental Science Technology*, 41, 998-1003.

Subiela, V.J., de la Fuente, J.A., Piernavieja, G. and Penate, B. (2009), 'Canary Islands Institute of Technology (ITC) experiences in desalination with renewable energies (1996-2008), *Desalination and Water Treatment*, 7, 220-235.

Thomson, M. and Infield, D. (2005), 'Laboratory demonstration of a photovoltaic-powered seawater reverse-osmosis system without batteries', *Desalination*, 183, 105-111.

Thomson, M. and Infield, D. (2002), 'A photovoltaic-powered seawater reverse-osmosis system without batteries', *Desalination*, 153, 1-8.

Thomson, M., Miranda, M.S. and Infield, D. (2002), 'A small-scale seawater reverse-osmosis system with excellent energy efficiency over a wide operating range', *Desalination*, 153, 229-236.

Tzen, E., Perrakis, K. and Baltas, P. (1998), 'Design of a stand alone PV-desalination system for rural areas', *Desalination*, 119, 327-334.

Weiner, D., Fisher, D., Moses, E.J., Katz, B. and Meron, G. (2001), 'Operation experience of a solar- and wind-powered desalination demonstration plant', *Desalination*, 137, 7-13.

Werner, M. and Schafer, A.I. (2007), 'Social aspects of a solar-powered desalination unit for remote Australian communities', *Desalination*, 203, 375-393.

Witte, T., Siegfriedsen, S. and El-Allawy, M. (2003), 'WindDeSalter® Technology; Direct use of wind energy for seawater desalination by vapour compression or reverse osmosis', *Desalination*, 156, 275-279.

APPENDIX A

Description of tests

The following is a description of all tests and the adjustments that were made to improve the operation of the system.

A.1 TEST 1

This test was the first using the artificial seawater and fluctuating operating conditions. The machine was stopped and flushed with 160L of DW water once a day, otherwise it ran continuously. During test 1 an external fan was added to the system directing air onto the HPP to avoid overheating when operating at slow speeds for extended periods. Also the conductivity readings were found to be inaccurate. This was found to be caused by air bubbles being trapped in the conductivity sensor housing. Changing the orientation of the conductivity sensor solved this problem, however the conductivity data for the first 25 hours of operation was discarded.

Operation of the machine was not consistent over the whole operating range and an audible 'knocking' sound was heard coming from the HPP at times, especially at the lower speed range. Varying the feed pressure via adjustments to the speed of the feed pump had short-term effects of reducing the noise, but it resumed after continuing fluctuating operation. Eventually test 1 was terminated due to the sustained 'knocking' noise at low pump speeds.

It was observed on day 5 of this test during the last flush, that a thin, fibrous material which appeared to be fragments of a biofilm, was discharged from the concentrate line.

A.2 TEST 2

In order to achieve smoother operation of the Pearson Pump, a program was entered into the computer such that the feed pump had two separate equations to control its speed. When the HPP was operating at a speed voltage below 7.6V, the feed pump would deliver water at around 0.8 bar while for speeds above 7.6V, the feed pressure would be 1.2 bar.

Test 2 was commenced using this revised program which appeared to remedy the previous concerns of excessive HPP noise. Later during this operating cycle, some large fluctuations in the wind speed data were encountered. During these events, the HPP again commenced the 'knocking' sound for a period until it adjusted to the fluctuation in operation. It was perceived that this was caused by the temporary imbalance in feed pressure, since both the feed pump and HPP change speeds at the same time. However, it takes a short time for the effect of the feed pump speed change to pass through to the pre-filter and feed line. To rectify this, a smoothing device was installed on day 2 of operation to provide a 5 second delay between the change of the feed pump and the high pressure Pearson Pump. This allowed for a smoother transition and reduced pump noise.

A further irregularity in operation was observed when the HPP operated for periods at a speed voltage of 7.6V. This is the speed at which the formula for the feed pump changes between its high and low range and since there are slight fluctuations in the speed voltage, the feed pump was found to be jumping between its two ranges. Additionally, a vibration in the HPP started to develop at higher pump speeds. On day 4 the test was terminated so the computer program could be adjusted to eliminate the aforementioned problem of the feed pump jumping between its high and low ranges.

A.3 TEST 3

An audible knocking sound persisted initially through Test 3; changing the feed pump pressure to a lower level seemed to stabilize operation before it was left to run overnight. Inspection of data from the machine the next day showed inconsistent operation with the product flow having a 'wave-like' appearance. Test terminated.

A.4 TEST 4

No useful data was generated from Test 4. Testing showed inaccurate readings from the product flow meter and this was assessed to be caused partly by electrical noise. A capacitor was added to the wiring of the product flow meter which improved the consistency of the readings, however the flow meter now seemed to be overestimating the flow rate by 7%.

A.5 TEST 5

During Test 5 the inaccuracy of the flow meter was confirmed and adjustments made to the data for this test. It is assumed the inaccuracy only developed at the end of Test 3 since the meter was calibrated at the beginning of the experiments.

The drinking water standard established by the World Health Organization (WHO) sets a limit of 500 mg/L TDS. The equivalent conductivity would be, using equation 1:

$$y = 0.5 / 0.65$$

$$= 0.770 \text{ mS/cm or } 770 \text{ µS/cm}$$

For Test 5 the range of operating speeds was narrowed to a higher range since none of the previous tests had achieved an average conductivity below the target of 770 µS/cm. Due to the raising of overall operating speeds of the HPP, it was perceived as necessary to add a potential meter between the computer speed signal and the HPP. This is due to the fact that the manufacturer of the membranes, DOW Filmtec, recommends a pressure increase in the membranes over a 30-60 second period (DOW website). In this way, after a freshwater flush, the speed of the HPP can be raised gradually with the potential meter while keeping the computer program running.

This test was terminated on Christmas eve and the system prepared to sit idle for 10 days over the holiday period. This involved running the regular DW flush followed by flushing the supply line and prefilter with 20 litres of the permeate from the DW flush. An additional 80 litres of DW was finally flushed through the system while the prefilter was removed, rinsed in DW and left out to dry. Fragments of biofilm were visible on the pre-filter indicating biofouling.

A.6 TEST 6

Test 6 trials were commenced after a 10 day idle period, and this involved initially flushing out the storage water in the membranes with the regular DW flush procedure. Following this, trials were run to retest the upper limit of the operating range of the Pearson Pump. It was found in these tests that the speed voltage could be increased up to a possible 10.4V, using an external voltage supply, before reaching the maximum available power of 900W.

The machine was initiated into a regular production cycle to run overnight. The following day Test 6 was terminated to reassess the product quality from the run cycles. None of the cycles so far had produced an average product quality of below the target 770 µS/cm (500 mg/L TDS) during a full day's production. To achieve this, the average speed of the HPP needed to be raised to increase the flux across the membrane and give a greater dilution in the permeate.

It was found that the potential meter used to regulate the speed of the HPP during stops in the cycle for fresh water flushes, also caused a resistance of 0.3V. The voltage signal from the computer has a maximum 10V output, however, with the resistance of the circuit this was only an effective 9.7V.

A.7 TEST 7

The potential meter was removed to obtain the maximum available speed of the pump. The effect of this was that now the pressure could not be raised manually after stopping the machine for a fresh water flush without terminating the cycle on the computer. Due to this, the program for the computer was re-written into 2 day blocks of data (days 2 & 3, 4 & 5, etc) such that the cycle would now run continuously for 2 days before being terminated, flushed with the standard DW procedure, restarted manually to raise the pressure in the membranes, then initiated into the next 2 day cycle. These cycles were then replicated to test the consistency of the operation (Test 7b). The replicated test showed results whose difference was within the 2% error range of the instrumentation, suggesting consistent data from the tests. A feed pressure of 0.8–1 bar gave the smoothest operation over the HPP speed range.

APPENDIX B

Determining relationships

B.1 HPP speed voltage vs. RPM

It was deemed necessary to establish a relationship between the speed voltage being used on the HPP and the revolutions per minute (RPM) of the pump motor. This was primarily due to correspondence had with the manufacturers of the HPP after unsatisfactory operation of the machine. The information received from the manufacturers quoted a range of operation using RPM as the indication of the speed of the pump. Since the machine was not fitted with such a device, a magnetic sensor was fitted temporarily to the fan cover of the high speed pump motor with a small bolt placed through a blade of the fan to count the revolutions. The signal was fed through an oscilloscope that gave a reading in Hertz which could then simply be multiplied by 60 seconds to give RPM. The speed of the HPP was adjusted manually in 0.5V increments and the RPM recorded for each speed voltage once the operation had stabilized. The results were then graphed (Figure B1) and the following formula was derived:

RPM = 125.66 * (SPEED V) – 254.74

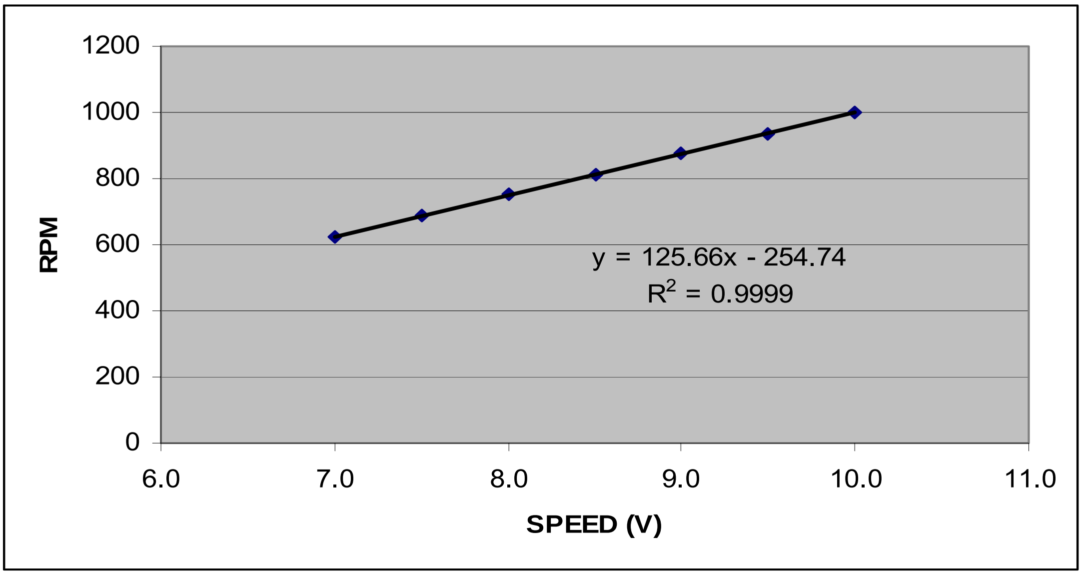

Figure B1: Determining relationship between RPM and HPP speed voltage.

B.2 HPP speed voltage vs. Power consumption

In order to estimate the consumption of power during production, a test was carried out similar to the procedure described above. However instead for each increment of speed voltage the voltage and current from the DC power source were recorded then multiplied together to determine power consumption in Watts. This was a strong relationship throughout the tests (Figure B2) determined as:

Watts = 128.59 * (SPEED V) – 448.53

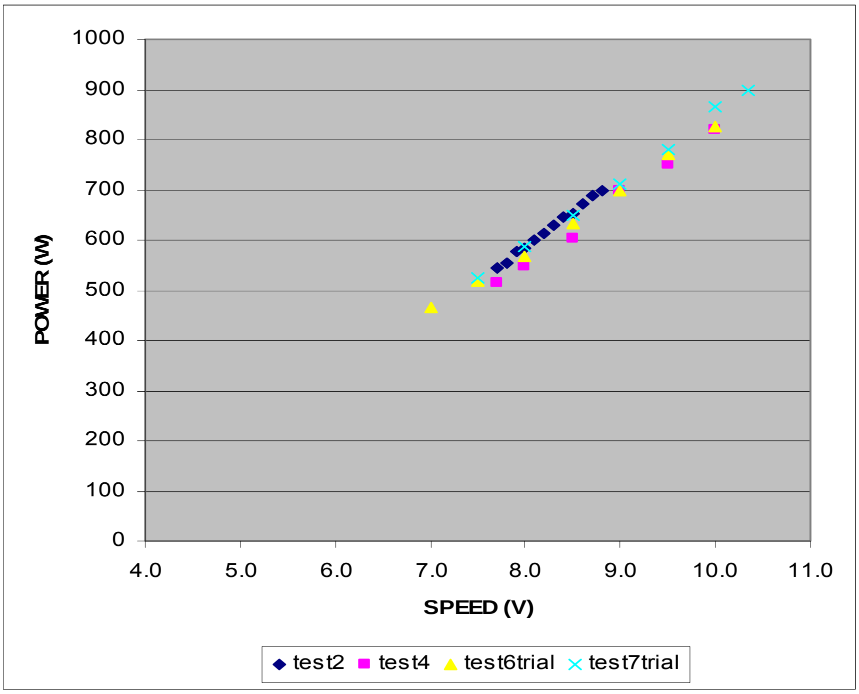

As can be seen in Figure B2 the relationship between power and speed of the HPP remains strong throughout the testing with the coefficient of determination (R^2) calculated to be 0.9786 using the trend line function of Microsoft Excel ®.

Figure B2: Determination of relationship between high pressure speed and power.